nature | **methods**

Mechanical regulation of cell function with geometrically modulated elastomeric substrates

Jianping Fu, Yang-Kao Wang, Michael T Yang, Ravi A Desai, Xiang Yu, Zhijun Liu & Christopher S Chen

Supplementary figures and text:

Supplementary Figure 1	Fabrication and characterization of micromolded elastomeric PDMS micropost arrays.
Supplementary Figure 2	Representative immunofluorescence images of hMSCs on the PDMS micropost arrays of different post heights.
Supplementary Figure 3	Correlative analysis of hMSC morphology and traction force during rigidity-sensing and mechanotransduction.
Supplementary Figure 4	Mechanical regulation of hMSC differentiation on micromolded PDMS micropost arrays.
Supplementary Figure 5	Commitment and differentiation of hMSCs towards osteogenesis requires sustained cytoskeletal contractility at the early stage.
Supplementary Figure 6	Bar graphs showing differentiation probability of single hMSCs towards either osteogenesis or adipogenesis as a function of the normalized traction force at groups of time points.
Supplementary Note 1	Statistical analysis of hMSC differentiation with contractility.

Nature Methods: doi: 10.1038/nmeth.1487

SUPPLEMENTARY FIGURES

Supplementary Figure 1

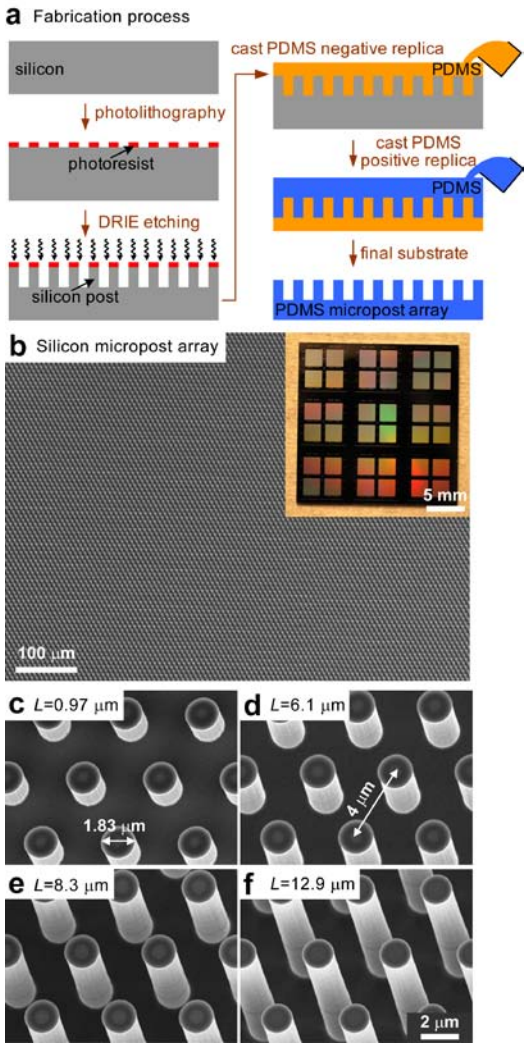

Supplementary Figure 1. Fabrication and characterization of micromolded elastomeric PDMS micropost arrays. (**a**) Fabrication of elastomeric PDMS micropost arrays involves standard photolithography and deep reactive-ion etching (DRIE) for the silicon micropost array masters in a cleanroom environment, and then replica molding with PDMS to generate the final PDMS micropost arrays. (**b**-**f**) Scanning electron microscopy images of microfabricated hexagonally arranged silicon micropost array masters with different post heights L as indicated. The silicon microposts have a diameter d of 1.83 μm, with a center-to-center spacing of 4 μm. L varies from 0.97 μm to 14.7 μm. The inset in (**b**) shows a photograph of the silicon micropost array master.

Nature Methods: doi: 10.1038/nmeth.1487

Supplementary Figure 2

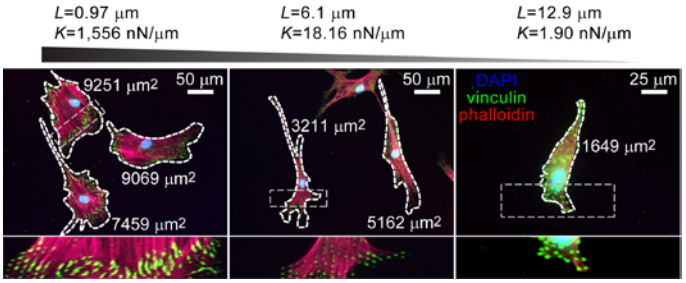

Supplementary Figure 2. Representative immunofluorescence images of hMSCs on the PDMS micropost arrays of different post heights. hMSCs were stained with fluorophore-labelled phalloidin, anti-vinculin, and DAPI to visualize actin filaments, FAs, and the nuclei, respectively. Dashed white lines highlight cell boundaries with cell spread areas indicated. Magnified views of the portions of the cells in the gray rectangles are shown in the bottom row. hMSCs were grown overnight in GM prior to fixation and immunostaining.

Nature Methods: doi: 10.1038/nmeth.1487

Supplementary Figure 3

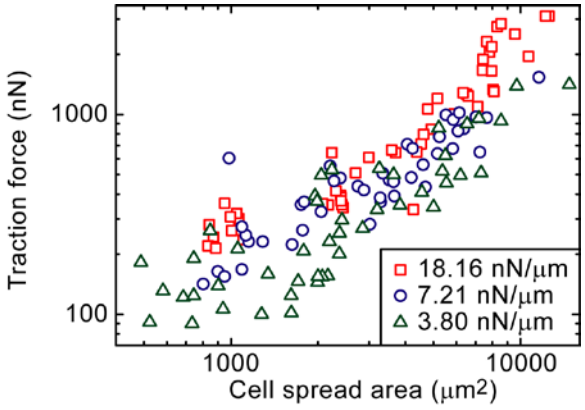

Supplementary Figure 3. Correlative analysis of hMSC morphology and traction force during rigidity-sensing and mechanotransduction. Total traction forces per single hMSCs are plotted as a function of hMSC spread area. Each data point represents an individual cell. Data are collected from three different PDMS micropost arrays (L = 6.1 μm, k = 18.19 nN/μm (□); L = 8.3 μm, k = 7.21 nN/μm (○); L = 10.3 μm, k = 3.80 nN/μm (△)).

Nature Methods: doi: 10.1038/nmeth.1487

Supplementary Figure 4

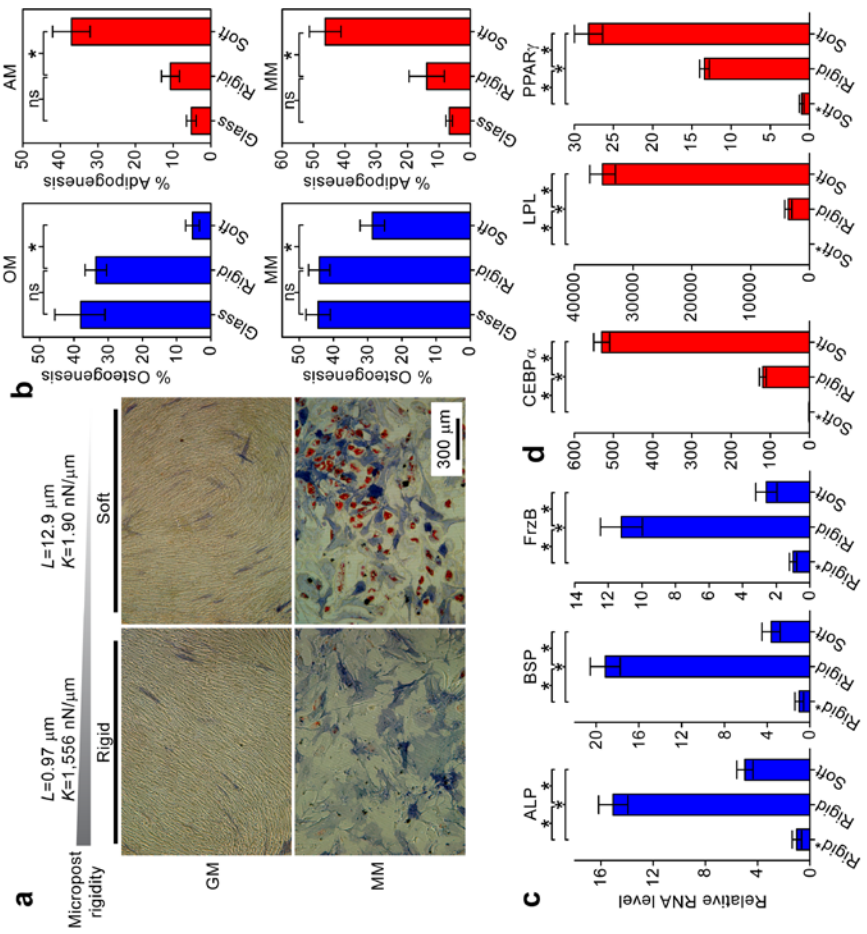

Supplementary Figure 4. Mechanical regulation of hMSC differentiation on micromolded PDMS micropost arrays. (**a**) Phase-contrast micrographs of hMSCs plated on the PDMS micropost arrays of different post heights (left: rigid, L = 0.97 μm, K = 1,556 nN/μm; right: soft, L = 12.9 μm, K = 1.90 nN/μm). hMSCs were stained for both alkaline phosphatase (ALP, *blue*) and fat lipids (Lip, *red*) after 14 days of culture in either GM (top panel) or MM (bottom panel). (**b**) Bar graphs showing percentage of differentiation of hMSCs towards either osteogenesis (left column) or adipogenesis (right column), after 14 days of culture in either OM (top left), AM (top right), or MM (bottom panel). Experimental data are presented as the mean of three or four independent experiments, and error bars represent ± s.e.m. (OM: *ns* (P = 0.595) and * (P = 4.1E-4); AM: *ns* (P = 0.0972) and * (P = 0.003); MM/Osteogenesis: *ns* (P = 0.952) and * (P = 0.0174); MM/Adipogenesis: *ns* (P = 0.329) and * (P = 0.0096); Student's t-test). Glass coverslips coated with fibronectin served as a control. (**c-d**) Osteogenic (**c**; ALP, bone sialoprotein (BSP), and frizzled B (FrzB)) and adipogenic (**d**; CCAAT-enhancer-binding protein alpha (CEBPα), lipoprotein lipase (LPL), and peroxisome proliferator-activated receptor gamma (PPARγ)) gene expression of hMSCs on micropost arrays of different rigidities, assessed by qRT-PCR after 7 days of culture in MM, plotted against micropost rigidity. For each gene, expression was normalized to cells cultured in GM on either rigid (**c**, *Rigid**) or soft PDMS micropost arrays (**d**, *Soft**). Error bars represent ± s.e.m. (n = 4) (*, P < 0.05; Student's t-test).

Nature Methods: doi: 10.1038/nmeth.1487

Supplementary Figure 5

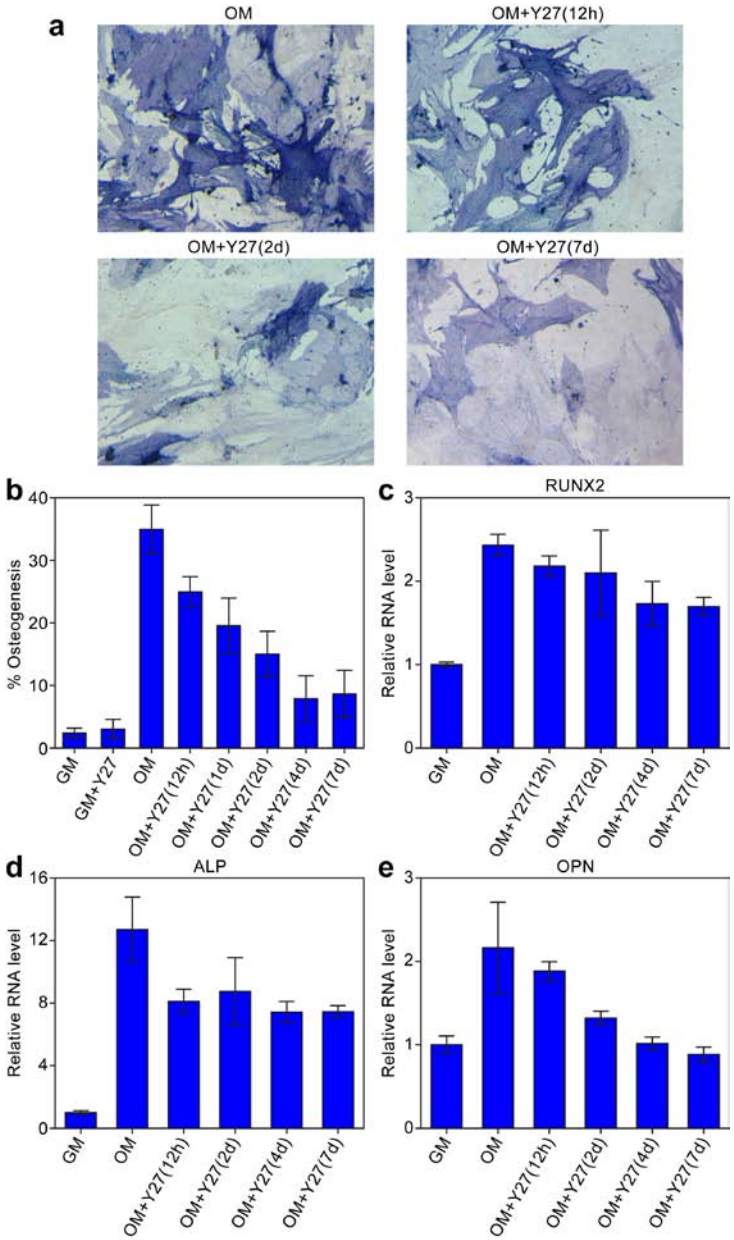

Supplementary Figure 5. Osteogenic differentiation of hMSCs requires sustained CSK contractility at the early stage. (**a**) Phase-contrast micrographs of hMSCs plated on glass coverslips. hMSCs were stained for ALP (*blue*) after 7 days of culture in OM. ROCK inhibitor Y27632 (Y27, 10 μM) was initially added to OM for different periods as indicated. (**b**) Bar graphs showing percentage of differentiation of hMSCs towards osteogenesis affected by Y27632 treatments. hMSCs were stained for ALP after 7 days of culture in either GM or OM. ROCK inhibitor Y27632 (10 μM) was initially added to GM or OM for different periods as indicated. (**c-e**) Osteogenic (runt-related transcription factor 2 (RUNX2), ALP, osteopontin (OPN)) gene expression of hMSCs assessed by qRT-PCR after 7 days of culture in either GM or OM were down-regulated by Y27632 treatments for different periods as indicated. For each gene, expression was normalized to cells cultured in GM. Error bars represent ± s.e.m. (n = 4).

Nature Methods: doi: 10.1038/nmeth.1487

Supplementary Figure 6

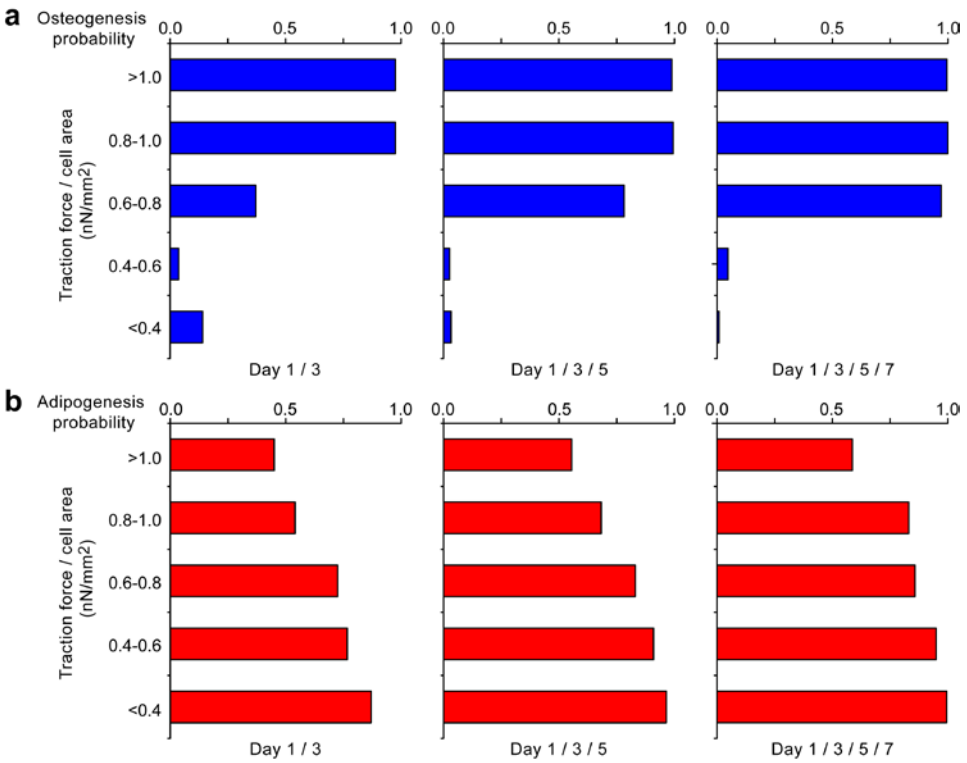

Supplementary Figure 6. Bar graphs showing differentiation probability of single hMSCs towards either osteogenesis (**a**) or adipogenesis (**b**) as a function of the normalized traction force at groups of time points (Day 1/3, Day 1/3/5 and Day 1/3/5/7). The probability for five different levels of *f* were calculated, from most contractile ($f > 1.0$) to least contractile ($f < 0.4$), using the naïve *Bayes* classifier analysis (**Supplementary Note**).

Nature Methods: doi: 10.1038/nmeth.1487

SUPPLEMENTARY NOTE

Statistical analysis of hMSC differentiation with contractility. Inferring hMSC differentiation from the early daily traction force levels was formulated as a classification problem[1,2]. We classified hMSC differentiation phenotypes Y into two classes (y_0 = ALP+ and y_1 = ALP- for osteogenesis; y_0 = Lip+ and y_1 = Lip- for adipogenesis), and assigned daily traction force levels $F = f_j$, where f_j represented one of the five traction force levels (in nN μm^{-2}) as

$$\begin{pmatrix} f_1 \\ f_2 \\ f_3 \\ f_4 \\ f_5 \end{pmatrix} \equiv \begin{pmatrix} F < 0.4, \\ 0.4 \le F < 0.6 \\ 0.6 \le F < 0.8 \\ 0.8 \le F < 1.0 \\ F \ge 1.0 \end{pmatrix}.$$

We defined the prior and posterior probabilities as the probabilities of hMSCs differentiating into each phenotype class before and after knowing the information of the daily traction force levels, respectively. The prior probabilities of each phenotype class are defined as

$$\begin{cases} P(ALP+) \equiv P(Y = y_0) \\ P(ALP-) \equiv P(Y = y_1) = 1 - P(Y = y_0) \end{cases} \quad \text{for osteogenesis,}$$

and

$$\begin{cases} P(Lip+) \equiv P(Y = y_0) \\ P(Lip-) \equiv P(Y = y_1) = 1 - P(Y = y_0) \end{cases} \quad \text{for adipogenesis.}$$

To estimate these probabilities, the Maximum Likelihood Estimate (MLE) method was applied with Laplace Smoothing (LS) as

$$\hat{\pi}_k = \hat{P}(Y = y_k) = \frac{\#D\{Y = y_k\} + 1}{|D| + K} \ (k = 1, 2; K = 2),$$

where the operator $\#D\{x\}$ reported the number of elements in the set D that satisfied property x[2]. Therefore, to perform statistical analysis for hMSC osteogenesis as an example, we could utilize the osteogenic dataset in **Fig. 3f**, and $\#D\{Y = y_0\}$ and $|D|$ would be the number of ALP+ cells and the total number of hMSCs in the dataset, respectively. According to the Bayes theorem, the posterior probability of hMSCs differentiating into each phenotype class given a specific daily traction force level was calculated as

$$P(Y = y_k \,|F = f_j) = \frac{P(Y = y_k) P(F = f_j \,|Y = y_k)}{\sum_{i=1}^{2} P(Y = y_i) P(F = f_j \,|Y = y_i)} \ (k = 1, 2;\ j = 1, 2, 3, 4, 5),$$

where $P(F = f_j|Y = y_k)$ was the likelihood of a specific daily traction force level in each phenotype class. $P(F = f_j|Y = y_k)$ was also estimated by MLE with LS as

$$\hat{\theta}_{jk} = \hat{P}(F = f_j \,|Y = y_k) = \frac{\#D\{F = f_j \wedge Y = y_k\} + 1}{\#D\{Y = y_k\} + J} (j = 1, 2, 3, 4, 5; k = 1, 2; J = 5).$$

Therefore, the probability that hMSCs would become ALP+ with the traction force level F on Day 1 in the range of $0.4 \le f < 0.6$ was calculated as

$$P(ALP+ \,|0.4 \le f_{Day1} < 0.6) = P(Y = y_1 \,|F_{day1} = f_2) = \frac{\hat{\pi}_1 \hat{\theta}_{21}}{\hat{\pi}_1 \hat{\theta}_{21} + \hat{\pi}_1 \hat{\theta}_{22}}.$$

Nature Methods: doi: 10.1038/nmeth.1487

We also calculated the posterior probability for hMSCs that maintained a constant contractility level across multiple days, where the daily traction force levels F were assumed conditionally independent from each other, a so-called naïve Bayes condition. Thus, the posterior probability for hMSCs that maintained a constant contractility level across multiple days was calculated as

$$P(Y = y_k \left| F_{day1}, F_{day3}, \ldots F_{day\,N} \right.) = \frac{P(Y = y_k)P(F_{day1} \left| Y = y_k \right.)P(F_{day3} \left| Y = y_k \right.)\ldots P(F_{day\,N} \left| Y = y_k \right.)}{\sum_{i=1}^{2} P(Y = y_i)P(F_{day1} \left| Y = y_i \right.)P(F_{day3} \left| Y = y_i \right.)\ldots P(F_{day\,N} \left| Y = y_i \right.)}$$

$(k = 1, 2)$.

REFERENCES OF SUPPLEMENTARY NOTE

1. Pe'er, D. *Science STKE* **2005**, pl4 (2005).
2. Mitchell, T.M. *Generative and Discriminative Classifiers: Naive Bayes and Logistic Regression* in *Machine Learning*, 2nd edn (draft of Sept., 2006, http://www.cs.cmu.edu/~tom/mlbook/NBayesLogReg.pdf).

Nature Methods: doi: 10.1038/nmeth.1487